Characterization of dielectric properties of polycrystalline aluminum nitride for high temperature wireless sensor nodes

S Knaust[1], Z Khaji[1], P Sturesson[2], and L Klintberg[1]

[1] Division of Microsystems Technology, Department of Engineering Sciences, Uppsala University, Uppsala, Sweden
[2] National Swedish Defence College, Stockholm, Sweden

E-mail: stefan.knaust@angstrom.uu.se

Abstract. An aluminium nitride (AlN) passive resonance circuit intended for thermally matched high temperature wireless sensor nodes (WSN) was manufactured using thick-film technology. Characterization was done for temperatures up to 900°C in both a hot-chuck for frequencies below 5 MHz, and using wireless readings of resonating circuits at 15 MHz, 59 MHz, and 116 MHz. The substrate for the circuits was sintered polycrystalline AlN. Using a simplified model for the resonators where the main contribution of the frequency-shift was considered to come from a shift of the dielectric constant for these frequencies, the temperature dependency of the dielectric constant for AlN was found to decrease with increasing frequency up to 15 MHz. With an observed frequency shift of 0.04% at 15 MHz, and up to 0.56% at 59 MHz over a temperature range of 900°C, AlN looks as a promising material for integration of resonance circuits directly on the substrate.

1. Introduction

To realize high-temperature wireless sensor nodes (WSN), e. g. for monitoring of components operating at temperatures above 300°C, polymer-based materials fall short because of their low temperature tolerance and large thermal expansion. Hence ceramic alternatives are worth considering. Single-crystalline aluminium nitride (AlN), being a wide band-gap semiconductor, has attracted recent attention as surface acoustic wave resonators used for sensors and energy harvesters [1, 2, 3], currently capable of generating energies up to 2 μW [4]. Although often designed to work at room temperature, AlN-based components could theoretically sustain its piezoelectric properties up to 1150°C [5]. However, for these wide temperature ranges, integration of components into sensor nodes, packaging and communication is still a challenge. Large temperature variations requires minimizing the thermal stresses from coefficient of thermal expansion (CTE) mismatch, and for most materials, the electrical properties will vary extensively with temperature.

To ensure a good CTE matching, a homogeneous system is preferred and to enable multicomponent systems, sintered AlN is a promising substrate material for high temperature applications with a close to perfect CTE match to crystalline AlN ($5.36{*}10^{-6}/K$, 20°C - 1000°C), and also to silicon carbide ($5.18{*}10^{-6}/K$, 20°C - 1000°C) [6]. Although showing rapidly increasing conductivity above 600°C , AlN remains a reasonably good insulator [7], and

together with a thermal conductivity (150 W/mK - 180 W/mK) [8] comparable to many metals, high corrosion resistance and good mechanical properties (Young´s modulus of 340 GPa, and flexural strength of 320 MPa) [9], AlN is considered as a suitable substrate material for harsh environments, both at high ambient temperatures and where the temperature is generated from attached components. Compared to the commonly used construction ceramic alumina, AlN has a higher resistance to thermal shock [10].

Although crystalline AlN is well characterized [11, 12], there are gaps to fill when it comes to understanding the properties of the sintered ceramic. In the 1960s, Taylor and Lenie characterized the drift of the dielectric constant for AlN up to 500°C [13], manufactured by hot isostatic pressure (HIP). Their AlN was reported to have 4% of impurities among which O, Si and Fe were present, giving characteristics comparable to alumina. Today, sintered AlN from major manufacturers like Maruwa and Sienna Technologies, the impurities, still about 5%, mainly consists of Y_2O_3. It is therefor of interest to verify the properties of the material.

2. Theory

For resonant circuits, the corresponding resonance frequency is

$$f = \frac{1}{2\pi\sqrt{LC}}, \tag{1}$$

where L is the inductance and C is the total capacitance in the circuit. The inductances of the loops depends primarily on the geometry [14]. Physical dimensions of the loop (the turning width, turning spacing and side size of the loop) are estimated to be linearly dependent on the CTE for AlN [6], giving rise to geometrical variations by approximately 0.5% over 1000°C. The influence of temperature on the inductance is small in comparison to the drift in capacitance, or more specific, the change in dielectric constant of the materials contributing to the capacitance, here dominated by the AlN parallel plate capacitor at the center of the passive antennas. Hence, the frequency will depend on temperature and dielectric constant according to

$$f \propto \frac{1}{\sqrt{\epsilon_{AlN}(T)}}. \tag{2}$$

3. Experimental

To evaluate the influence of temperature to the dielectric constant, three different resonance circuits were manufactured using 1 mm thick polycrystalline AlN substrates, ST-170, Sienna Technologies. Using silver thick-film paste, CN33-145, Ferro, single layers were printed and fired on both sides of the AlN substrate, and manually connected over the edges by a third deposition of silver paste, Figure 1. On the top side, the pattern consisted of a coil with the capacitor patch in the middle, and on the bottom side, the pattern consisted of only the patch for the capacitor.

The AlN in between the two printed parallel plates was used as a dielectric material for the resonating circuit, and the corresponding resonance frequencies were simulated to be close to 14 MHz, 60 MHz and 120 MHz, using Advanced Design System 2011.10. The simulated inductances of the antennas were 6 μH, 2 μH, and 1 μH, respectively.

To evaluate the devices, they were placed on a heating stage made out of an etched Kanthal foil acting as a heater having AlN plates as electrical insulators. The heating stage was placed in an alumina muffle that provided thermal insulation. To minimize the interference from the metal in the heater, the Kanthal foil was patterned in shape of a 2-dimensional torus, having a free area of only AlN below where the passive antennas were placed. The devices were monitored with respect to frequency shifts using a loop antenna outside of the muffle, actively powered through a vector network analyzer FieldFox N9923A, Agilent Technologies. To be able to match the large frequency span of the passive antennas, two different active loop antennas were used.

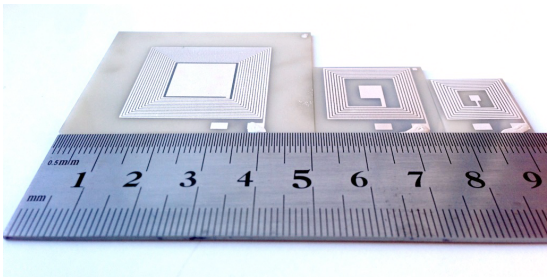

Figure 1. Fabricated silver-patterned, AlN-based inductively coupled antennas with the sizes of 3 x 3 cm^2 for 15 MHz, 2.5 x 2.5 cm^2 for 59 MHz, and 1.5 x 1.5 cm^2 for 116 MHz. Opposite to the patch in the middle of the chip, a patch is printed on the backside with the same dimensions, serving as a parallel plate capacitor for the circuit.

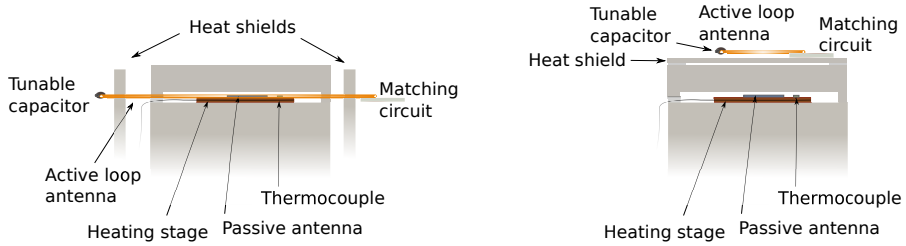

Figure 2. A cross sectional view of the setup. *(left)* The passive antenna is placed on a heating stage next to a thermocouple inside an alumina fixture. The passive antenna is read by an loop antenna consisting of a copper tube in series with a tunable capacitor, protected from thermal radiation by an alumina heat shield. *(right)* The smaller loop antenna was placed on top of the alumina fixture, centered above the passive antenna. An additional alumina sheet was placed in between the two antennas to provide protection from thermal radiation.

The large loop for readings below 20 MHz was placed around the alumina muffle, Figure 2 (left), and the smaller loop for higher frequencies was placed on top of the muffle, with an additional heat shield in between, Figure 2 (right), in order to keep the loops as close to room temperature (RT) as possible.

To account for the different resonance frequencies of the passive antennas, a variable capacitor was used to tune the active antenna. The stage temperature was varied between RT and 900°C using a constant increase of power, and the scattering parameter S11 was logged continuously. Having logged the frequency shifts and simulated the inductances, equation (2) can be used to calculate the changes of the dielectric constant.

As a complementary method for determining the dielectric constant of AlN for frequencies below 5 MHz, a 1 cm^2 plate capacitor manufactured with same material and process, was characterized on a hot- chuck connected to a B1500A, Aglient Technologies, parameter analyzer. The maximum applicable frequency was limited to 5 MHz and the maximum temperature was 600°C. Passive antennas for these low frequencies would have needed to be very large. Hence, no overlapping measurements could be conducted.

4. Results

The resonance frequencies of the passive antennas were measured to 15 MHz, 59 MHz, and 116 MHz, respectively. Figure 3 illustrates the relative frequency shift of the antennas over a

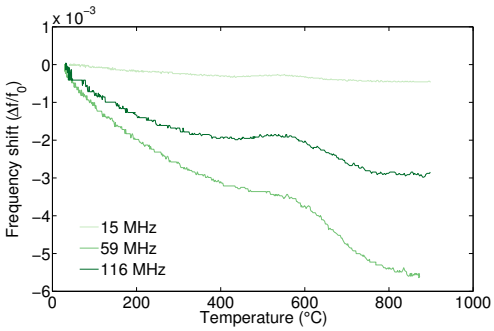

Figure 3. The frequency shift of the S11 signal versus temperature at readings for 15 MHz, 59 MHz, and 116 MHz.

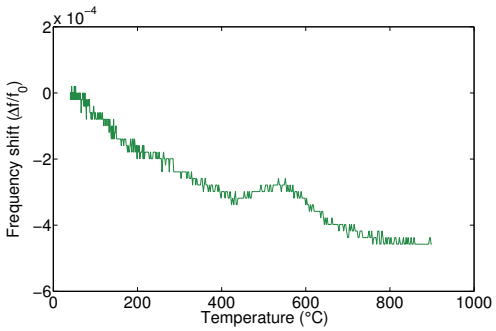

Figure 4. The frequency shift of the 15 MHz antenna versus temperature.

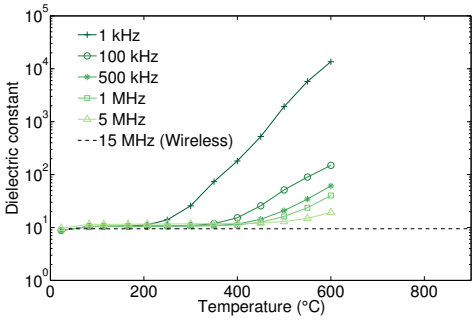

Figure 5. Dielectric constant for sintered AlN, measured in a hot-chuck probe station up to 600°C for frequencies in the range of 1 kHz to 5 MHz, and using wireless reading for 15 MHz. The temperature stability of the dielectric constant is seen to increase with frequency.

temperature range of 900°C. The same pattern for frequency shift was observed for all the three antennas, with decreasing values up to 400°C. Between 400°C and 550°C there is a plateau and above 550°C the frequency shift decreases again with slightly different rate. The 15 MHz reading was found to be most stable with a shift of only 7 kHz (0.04%) from RT to 900°C, Figure 4. This can be compared with an overall shift of 330 kHz (0.56%) and 352 kHz (0.28%) for 59 MHz and 116 MHz, respectively.

The dielectric constants extracted from the hot chuck measurement were found to be relatively constant up to 200°C where they started to increase rapidly, Figure 5. With increasing frequencies, the dielectric constant was observed to be more stable at higher temperatures. For the dielectric constant extracted for 15 MHz, only a small shift from 9.46 to 9.47 was measured, accounting for the thermal expansion of AlN over 900°C.

5. Discussion

Through out all measurements, a plateu is observed between 400°C and 600°C. This is believed to be caused by a sudden increase in conductivity for the AlN because of impurities, as reported by Francis and Worrell [7].

The approximation that the parallel plate capacitor dominates for the circuit is a simplification. For lower frequencies with large capacitance patches in the middle, other capacitive sources will not be significant. But for high frequencies with smaller patches, the

total capacitance is much more complex, including the addition of e. g. overlapping tracks and neighboring lines, giving stray capacitances of comparable magnitude, and the simplified model will be invalid. Hence, for the higher frequencies, the dielectric constant was not extracted.

For the higher frequencies, the active loop antenna had to be placed on top of the muffle, close to the heat source because of the lower reading ranges. At the highest temperatures, the temperature sensitive variable capacitor used for tuning was heated up to 50°C , resulting in a large drift in the measurements as seen in Figure 3 for 59 MHz and 116 MHz. For 15 MHz, a more stable variable capacitor was used which also was more successfully cooled. Hence, a more stable measurement was acquired.

6. Conclusion

Having small shifts over a temperature range of 900°C, the approach of integrating resonance circuits directly in an AlN substrate for use in high temperature wireless sensor nodes looks promising, with increasing stability for higher frequencies.

Acknowledgments

The authors would like to acknowledge the Knut and Alice Wallenberg foundation for financing the equipment.

References

[1] Yen T T, Hirasawa T, Wright P K, Pisano A P and Lin L 2011 *J. Micromech. Microeng.* **21**
[2] Tadigadapa S and Mateti K 2009 *Meas. Sci. Technol.* **20**
[3] Elfrink R, Kamel T M, Goedbloed M, Matova S, Hohlfeld D, van Andel Y and van Schaijk R 2009 *J. Micromech. Microeng.* **19**
[4] Saadon S and Sidek O 2011 *Energy Convers. Manage.* **52** 500–504
[5] Damjanovic D 1998 *Curr. Opin. Solid State Mater. Sci* **3** 469–473
[6] Werdecker W and Aldinger F 1984 *IEEE Trans. Compon., Hybrids, Manuf. Technol.* **7** 399 – 404
[7] Francis R W and Worrell W L 1976 *J. Electrochem. Soc.* **123** 430 – 433
[8] Coppola L, Huff D, Wang F, Burgos R and Boroyevich D 2007 Power Electronics Specialists Conference (IEEE) pp 2234 – 2240
[9] Boch P, Glandus J C, Jarrige J, Lecompte J P and Mexmain J 1982 *Ceram. Int.* **8** 34 – 40
[10] Lu T J and Fleck N A 1998 *Acta mater.* **46** 4755 – 4768
[11] Cimalla V, Pezoldt J and Ambacher O 2007 *J. Phys. D: Appl. Phys.* **40** 1–50
[12] Willander M, Friesel M, ul Wahab Q and Straumal B 2006 *J. Mater. Sci. - Mater. Electron.* **17** 1–25
[13] Taylor K M and Lenie C 1960 *J. Electrochem. Soc.* **107** 308–314
[14] Greenhouse H M 1974 *IEEE Trans. Parts, Hybrids, Packag.* **10** 101 – 109